
The Translocator Protein Radioligand ^{18}F -DPA-714 Monitors Antitumor Effect of Erufosine in a Rat 9L Intracranial Glioma Model

Ali R. Awde^{1,2}, Raphaël Boisgard^{1,2}, Benoit Thézé^{1,2}, Albertine Dubois^{1,2}, Jinzi Zheng^{1,2}, Frédéric Dollé¹, Andreas H. Jacobs³, Bertrand Tavitian^{1,2,4}, and Alexandra Winkeler^{1,2}

¹CEA-DSV-I2BM-SHFJ, Orsay, France; ²Inserm U1023, Laboratoire d'Imagerie Moléculaire Expérimentale, Université Paris Sud, Orsay, France; ³Westfälische-Wilhelm-University Münster (WWU), European Institute for Molecular Imaging, Münster, Germany; and ⁴Inserm U970, PARCC, Université Paris Descartes, Hôpital Européen Georges Pompidou, Paris, France

On the one hand, the translocator protein (TSPO) radioligand *N,N*-diethyl-2-(2-(4-(2- ^{18}F -fluoroethoxy)phenyl)-5,7-dimethylpyrazolo [1,5-*a*]pyrimidin-3-yl)acetamide (^{18}F -DPA-714) has been suggested to serve as an alternative radiotracer to image human glioma, and on the other hand the alkylphosphocholine erufosine (ErPC3) has been reported to induce apoptosis in otherwise highly apoptosis-resistant glioma cell lines. The induction of apoptosis by ErPC3 requires TSPO, a mitochondrial membrane protein highly expressed in malignant gliomas. In this preclinical study, we monitored the effect of ErPC3 treatment *in vivo* using ^{18}F -DPA-714 PET. **Methods:** *In vitro* studies investigated the antitumor effect of ErPC3 in 9L rat gliosarcoma cells. *In vivo*, glioma-bearing rats were imaged with ^{18}F -DPA-714 for the time of treatment. **Results:** A significant decrease in 9L cell proliferation and viability and a significant increase in apoptosis and caspase-3 activation were demonstrated on ErPC3 treatment in cell culture. In the rat model, ErPC3 administration resulted in significant changes in ^{18}F -DPA-714 tumor uptake over the course of the treatment. Immunohistochemistry revealed reduced tumor volume and increased cell death in ErPC3-treated animals accompanied by infiltration of the tumor core by CD11b-positive microglia/macrophages and glial fibrillary acidic protein-positive astrocytes. **Conclusion:** Our findings demonstrate a potent antitumor effect of ErPC3 *in vitro*, *in vivo*, and *ex vivo*. PET imaging of TSPO expression using ^{18}F -DPA-714 allows effective monitoring and quantification of disease progression and response to ErPC3 therapy in intracranial 9L gliomas.

Key Words: glioma; ErPC3; TSPO; ^{18}F -DPA-714

J Nucl Med 2013; 54:2125–2131

DOI: 10.2967/jnumed.112.118794

The 18-kDa translocator protein (TSPO) is a mitochondrial membrane protein implicated in cholesterol transport, cell proliferation, and apoptosis (1). TSPO is mainly located in the adrenal glands, kidneys, lungs, and heart. It has a low expression level

in the central nervous system. However, TSPO expression is dramatically increased after glial cell activation and has become a well-characterized marker for neuroinflammation (2,3). TSPO overexpression has also been described in several human tumors, including breast, prostate, colon, and brain (4). Its overexpression is correlated with an aggressive tumor phenotype, increased cancer cell proliferation, and highly malignant tumor grades (5,6). In glioma, the overexpression of TSPO is associated with tumor cell proliferation, invasion, and migration (7,8).

PET is the preferred modality to noninvasively image and quantify TSPO expression in the brain and has been extensively performed in the past using the isoquinoline derivative ^{11}C -PK11195 in patients and animal models (9). Recently, newly developed TSPO radioligands with improved *in vivo* specificity for TSPO have been described. In particular, ^{18}F -DPA-714 (*N,N*-diethyl-2-(2-(4-(2- ^{18}F -fluoroethoxy)phenyl)-5,7-dimethylpyrazolo [1,5-*a*]pyrimidin-3-yl)acetamide (10)) has shown clear and quantitative PET imaging of TSPO expression in several animal models (11). Our group and others have successfully shown highly specific TSPO imaging using ^{18}F -DPA-714 in rat models of brain cancer and demonstrated its potential as a promising imaging marker for glioma (12,13). In addition, several studies have reported a correlation between TSPO protein levels measured using Western blot and TSPO radioligand binding (^3H -PK11195, ^{18}F -DPA-714, ^{18}F -PBR06) in rat models of glioma and multiple sclerosis (11,13–15).

Erucylphosphocholine (ErPC) is an alkylphosphocholine, part of a new class of synthetic lipophilic ether lipids that have shown promising antineoplastic activity *in vitro* and *in vivo* (16). ErPC demonstrated antitumor activity in several human and rat glioma cell lines (17,18) and induced apoptosis in the chemoresistant glioblastoma cell lines (15). Erucylphosphocholine (ErPC3; Erufosine [Genzyme]) is a congener of ErPC with higher water solubility and is able to cross the blood–brain barrier (19,20). Similarly to ErPC, ErPC3 exhibits potent antitumor activities in the micromolar range (21) and induces apoptosis in otherwise highly apoptosis-resistant glioblastoma cell lines (15). The mechanism of the cytotoxic and apoptotic actions of ErPC3 in several different cancer cell types has been linked to plasma membrane damage and direct or indirect disruption of Akt signaling (22). It has been suggested that ErPC3 could act directly on the mitochondria (23) because ErPC- and ErPC3-induced apoptosis require the presence of TSPO (24).

The present investigation focuses on characterizing the antineoplastic activity of ErPC3 in glioblastoma. Given the reported

Received Dec. 20, 2012; revision accepted Jul. 9, 2013.

For correspondence or reprints contact: Alexandra Winkeler, Laboratoire d'Imagerie Moléculaire Expérimentale, InsermU1023, CEA-DSV-I2BM-SHFJ, 4 Place du Général Leclerc, 91400 Orsay, France.

E-mail: alexandra.winkeler@cea.fr

Published online Nov. 8, 2013.

COPYRIGHT © 2013 by the Society of Nuclear Medicine and Molecular Imaging, Inc.

ability of ^{18}F -DPA-714 to accurately reflect TSPO density in normal or diseased brain (11,13), we investigated its performance to noninvasively and quantitatively assess treatment efficacy of ErPC3 in vivo in an orthotopic 9L glioma model. In addition, histologic and immunohistochemical analyses were used to evaluate the changes in tumor volume, intratumoral level of TSPO expression, and presence of TSPO-positive microglia/macrophages and astrocytes in ErPC3- and mock-treated animals.

MATERIALS AND METHODS

Assessment of Cell Viability, Proliferation, and Apoptosis

Rat 9L gliosarcoma cells were grown in Dulbecco modified Eagle medium (Sigma-Aldrich) containing 10% fetal bovine serum (Roche Diagnostics) and 1% antibiotics (penicillin/streptomycin; Life Technologies). Cultures were maintained at 37°C in humidified air containing 5% CO_2 .

Cell survival was assessed using the methyl-thiazoldiphenyl-tetrazolium bromide (MTT) assay (Sigma-Aldrich). 9L cells were plated at a density of 2.5×10^3 cells per well in 96-well microplates and incubated for 24, 48, 72, and 92 h with increasing concentrations of ErPC3 (0, 10, 25, 50, and 100 μM). ErPC3 was generously provided by Genzyme Pharmaceuticals. For in vitro studies, ErPC3 was dissolved in 70% ethanol and added to the cell culture medium at the desired final concentration. The ErPC3-containing medium was then removed and cells incubated for 1 h at 37°C with MTT in phosphate-buffered saline (5 mg/mL). After removal of the MTT solution, dimethyl sulfoxide (Sigma-Aldrich) was added for 15 min before absorbance values were determined using a Mithras Microplate Reader LB 940 (Berthold Technologies) at a 560-nm wavelength (reference wavelength, 650 nm). DNA synthesis was measured 24 h after the addition of ErPC3 by bromodeoxyuridine incorporation using the bromodeoxyuridine enzyme-linked immunosorbent assay (ELISA) kit (Roche Molecular Biochemicals) according to the manufacturer's instruction.

The Cell Death Detection ELISA Kit (Roche Molecular Biochemicals) was used to determine apoptosis (DNA fragmentation) in 9L cells treated with ErPC3 at concentrations of 0, 25, 50, and 100 μM . Cells (5.0×10^5) were plated in 6-well plates. Twenty-four hours after the addition of ErPC3, the cells were trypsinized, collected from the wells, and centrifuged (1,500g, 5 min, 4°C). Cell pellets were then resuspended in lysis buffer and treated according to the manufacturer's instruction. Absorption of the samples was measured at a wavelength of 405 nm (reference wavelength, 490 nm) using the Mithras Microplate Reader LB 940.

Western Blot

Western blots were performed as previously described (12) using the following primary antibodies: rabbit antirat TSPO antibody NP155 (provided by Dr. Makoto Higuchi, NIRS; 1/10,000 dilution), mouse antitubulin (Sigma-Aldrich; 1/20,000), rabbit anticaspase3 primary antibody (Cell Signaling Technology; 1/500), and appropriate secondary horseradish peroxidase-coupled antibodies (Santa Cruz Biotechnology; 1/2,000). More details are provided in the supplemental information (supplemental materials are available at <http://jnm.snmjournals.org>).

Animal Model

All experiments were performed under an animal use and care protocol approved by the local animal ethics committee and conducted in accordance with the European Union regulations on animal research. 9L gliosarcoma cells were stereotactically implanted in the brain of adult male Fischer rats (mean body weight, 301 ± 16 g; $n = 19$) as previously described (12). Glioma development was monitored using ^{18}F -DPA-714 PET. A baseline ^{18}F -DPA-714 PET scan was obtained 11 d after tumor implantation, and follow-up ^{18}F -DPA-714

PET scans were then acquired at 1 and 2 wk after therapeutic intervention. Rats received either ErPC3 (40 mg/kg of body weight, $n = 10$) or mock treatment (2% 1,2-propanediol diluted in saline, $n = 9$) at 48-h intervals up to 2 wk. For in vivo administrations, ErPC3 was prepared as described in the literature (20).

Radiochemistry

Ready-to-inject, radiochemically pure ^{18}F -DPA-714 (>99%) was prepared from cyclotron-produced ^{18}F -fluoride as previously reported (10) using a commercially available TRACERLab FX-FN synthesizer (GE Healthcare), a process that was formerly performed on a Zymate-XP robotic system (Zymark) (supplemental information) (25). The specific radioactivity of ^{18}F -DPA-714 samples used for this study was 120 ± 92 GBq/ μmol , with a range from 41 to 244 GBq/ μmol .

PET Imaging and Data Analysis

Brain imaging was performed on a Focus 220 micro-PET scanner (Siemens Medical Solutions). Animals ($n = 19$) were imaged at 11, 19, and 25 d after stereotactic implantation of 9L cells corresponding to 0, 8, and 14 d after intraperitoneal treatment. Rats receiving intravenous injections of ErPC3 were imaged at days 11, 18, and 25 after tumor implantation corresponding to 0, 7, and 14 d after treatment. Animals were anesthetized with an isoflurane/ O_2 mixture (induction, 4%–5%; maintenance, 2%–2.5%). During imaging, the head of the animals was fixed in the flat skull position using a homemade stereotactic frame compatible with PET acquisition. Their body temperature was maintained normothermic using a heating blanket. The PET radiotracer ^{18}F -DPA-714 was injected intravenously via a 24-gauge catheter placed on the tail vein. ^{18}F -DPA-714 injected doses were 53 ± 13 MBq. PET acquisition started 30 min after the injection of ^{18}F -DPA-714 and lasted 30 min (2 frames of 15-min acquisitions each). Finally, the emission sinograms for each acquisition frame were normalized and corrected for scatter, attenuation, and radioactivity decay. Image reconstruction was performed using Fourier rebinning and a 2-dimensional ordered-subset expectation maximization algorithm (16 subsets and 4 iterations).

PET image analysis was performed using VINCI, a fast graphical image analysis package (26) equipped with image coregistration tools, and the Anatomist BrainVISA software package (<http://www.brainvisa.info>). Quantitative volume-of-interest (VOI) analysis was performed on the summed image datasets. Briefly, a VOI was manually delineated on the tumor and, as a control region, a mirror reference VOI was symmetrically generated on normal brain tissue of the contralateral hemisphere as previously described (12).

Histology

After the last PET session, the rats were sacrificed and their brains rapidly excised and frozen in isopentane precooled in liquid nitrogen (-50°C) and then stored at -80°C until use. Frozen transversal brain sections (20- μm thick) of whole tumor specimen were cut at -20°C using a cryostat (Leica).

Brain sections were stained with hematoxylin and eosin according to the manufacturer's instructions (Labonord). Hematoxylin and eosin staining was used to estimate tumor volumes with the CellProfiler image analysis software (www.cellprofiler.org) (27). Tumor areas in coronal sections (20- μm thick) were delineated in every slice, and the total tumor volume was calculated according to Equation 1, where y_i is the cross-sectional area of the i^{th} section through the morphometric region, x_i is the distance orthogonal to the plane of section of the i^{th} section, and n is the total number of sections. Brain tumor sections (48 ± 8 per animal) were used to calculate tumor volume.

$$V_{\text{Runequal}} = \sum_{i=1}^{n-1} (x_{i+1} - x_i)(y_i) \quad \text{Eq. 1}$$

Immunohistochemistry staining was performed as previously described (supplemental information) (12). Sections were imaged using an AxioObserver Z1 microscope (Zeiss).

A terminal deoxynucleotidyl transferase-mediated dUTP nick-end labeling (TUNEL) assay was performed according to the manufacturer's instructions (DeadEnd Fluorometric TUNEL system; Promega). Negative controls were prepared by omitting nucleotides from the reaction mixture. These sections were subsequently incubated with rabbit anti-rat TSPO (NP155, 1:1000) and 4',6-diamidino-2-phenylindole as previously described. Specifically, the number of TUNEL-positive cells within the tumor area was assessed by estimating the percentage of labeled cells at 2 wk after treatment. Images were analyzed using the ImageJ software ((28); <http://rsbweb.nih.gov/ij/>). A region of interest (ROI) was manually defined for the areas showing positive TUNEL staining, and a second ROI was drawn based on the positive TSPO staining, which served as a surrogate marker for identifying the tumor area (12). The mean and SD of the ratio (TUNEL-positive areas/TSPO-positive tumor areas) were calculated, expressed in percentage, and used as the apoptotic index measured at 2 wk after treatment.

Autoradiography and competitive binding was used to assess specific binding for TSPO with an excess of unlabeled DPA-714 as previously described (supplemental information) (29). Autoradiograms were analyzed using the ImageJ software. ROIs were manually drawn on the tumor, and a control ROI was defined in the contralateral hemisphere. The mean greyscale value of each ROI in autoradiograms was expressed as the ratio of integrated density in arbitrary units per mm².

Statistical Analysis

Comparisons of cell culture data, PET data, and body weight assessment between control and treated animals were performed using a 1-way variance analysis and Bonferroni multiple comparison tests for post hoc analysis (GraphPad Prism; GraphPad Software Inc.). Two-group comparison was evaluated by an unpaired *t* test.

RESULTS

ErPC3 Inhibits Proliferation, Reduces Cell Viability, and Induces Apoptosis in 9L TSPO-Expressing Glioma Cells

Western blot analysis revealed high levels of TSPO proteins in rat 9L and C6 cells, whereas little or no TSPO signal was visible in murine GL261 cells (Fig. 1A).

Increasing inhibition of bromodeoxyuridine incorporation was observed in 9L cells after ErPC3 treatment at concentrations

ranging from 10 to 100 μ M (Fig. 1B, $***P < 0.001$ control vs. 25, 50, and 100 μ M ErPC3), whereas no effect on DNA synthesis was observed using a control solution. In addition, MTT assays showed a dose- and time-dependent toxicity on ErPC3-treated 9L cells (Fig. 1C) resulting in a significant reduction of cell viability already at 10 μ M and 24 h of ErPC3 administration ($P < 0.001$).

To determine whether the decrease in proliferation was due to apoptosis, we investigated ErPC3-induced DNA fragmentation and cleavage of caspase-3. 9L cells displayed a 2.0- up to 10.8-fold increase in apoptotic levels (at 10 and 100 μ M ErPC3, respectively; Fig. 2A). The augmentation of apoptotic levels was statistically significant ($P < 0.001$). Cleavage of caspase-3 was detected in ErPC3-treated cells as demonstrated by a decrease in the full-length protein and an increase in the level of cleaved caspase-3 (Fig. 2B).

ErPC3 Treatment of Intracranial 9L Glioma in Rats

Baseline PET images showed 3- to 4-fold-higher ¹⁸F-DPA-714 uptake in the tumor than in the control region ($P < 0.0001$ for ErPC3- and control-treated animals; Fig. 3A). Analysis of the PET data showed a decrease of ¹⁸F-DPA-714 uptake within the tumor, with respect to pretreatment uptake, at 8 and 14 d after initiation of ErPC3 treatment. In ErPC3-treated animals, the mean standardized uptake value (SUV) within the tumor VOI was 1.04 ± 0.21 (SUV range, 0.75–1.25, baseline), 1.14 ± 0.11 (0.98–1.22, day 8 after therapy), and 1.00 ± 0.18 (0.82–1.17, day 14 after therapy). In control animals, the SUV of ¹⁸F-DPA-714 uptake was 1.37 ± 0.15 (SUV range, 1.22–1.54, baseline), 1.77 ± 0.44 (1.21–2.16, day 8), and 1.55 ± 0.19 (1.34–1.78, day 14). The differences between groups were significant at 8 d of therapy ($P = 0.002$).

Intraperitoneal ErPC3 treatment, compared with control treatment, showed statistically significant loss of body weight ($P < 0.001$). Animals that received ErPC3 intraperitoneally showed a mean loss in body weight of $10.6\% \pm 1.2\%$ after 6 d of treatment. To investigate whether another administration route had less influence on body weight loss, we injected ErPC3 intravenously. Compared with controls, intravenously injected animals showed a significant mean reduction ($6.4\% \pm 1.9\%$) of body weight ($P < 0.001$). Loss of body weight was significantly higher for animals that received ErPC3 intraperitoneally than for those that received the drug intravenously ($P < 0.01$; Fig. 3).

To account for changes in body weight and ¹⁸F-DPA-714 uptake in the tumor versus a control region, normal brain of the contralateral hemisphere, tumor-to-normal brain ratios (T/NB) were calculated (Fig. 3). Even though the statistical significance of the difference between the 2 groups was reduced ($P < 0.05$) at 8 d after intraperitoneal ErPC3 administration, the T/NB values were 2.9 ± 0.6 and 4.7 ± 1.0 for ErPC3-treated versus mock-treated animals, respectively. Similar results were obtained for animals that received ErPC3 intravenously, with T/NB values of 2.9 ± 0.5 for ErPC3-treated and 5.3 ± 1.4 for control animals ($P < 0.01$).

Effect of ErPC3 on 9L Tumor Size, ¹⁸F-DPA-714 Binding, Apoptosis, and Cell Infiltration

The mean tumor volumes estimated from sections of whole tumor specimens

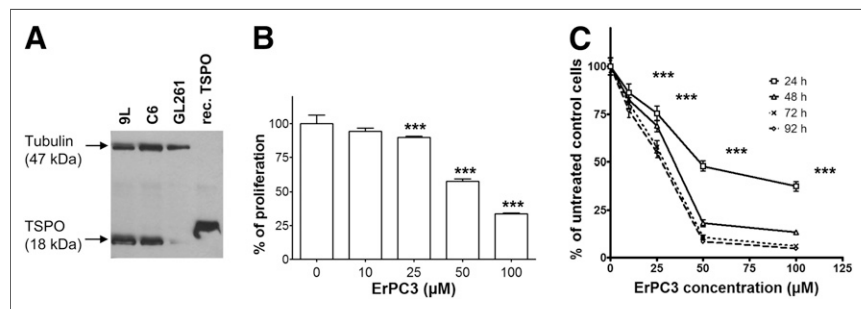


FIGURE 1. Expression levels of TSPO and effect of ErPC3 treatment on proliferation and viability of glioma cells in culture. (A) TSPO expression levels assessed by Western blot analysis of 9L, C6, and GL261 cells. β -tubulin was used as protein-loading index. TSPO recombinant protein has a molecular weight of 20.4 kDa, slightly larger than native TSPO. (B) Effect of ErPC3 on 9L cell proliferation as measured by bromodeoxyuridine incorporation. $***P < 0.001$ for 25, 50, and 100 μ M ErPC3 versus control. (C) Effect of ErPC3 on 9L cell viability using MTT assay. $***P < 0.001$, ErPC3- versus control-treated cells, 24 h. Results are expressed as mean \pm SD percentage of untreated controls.

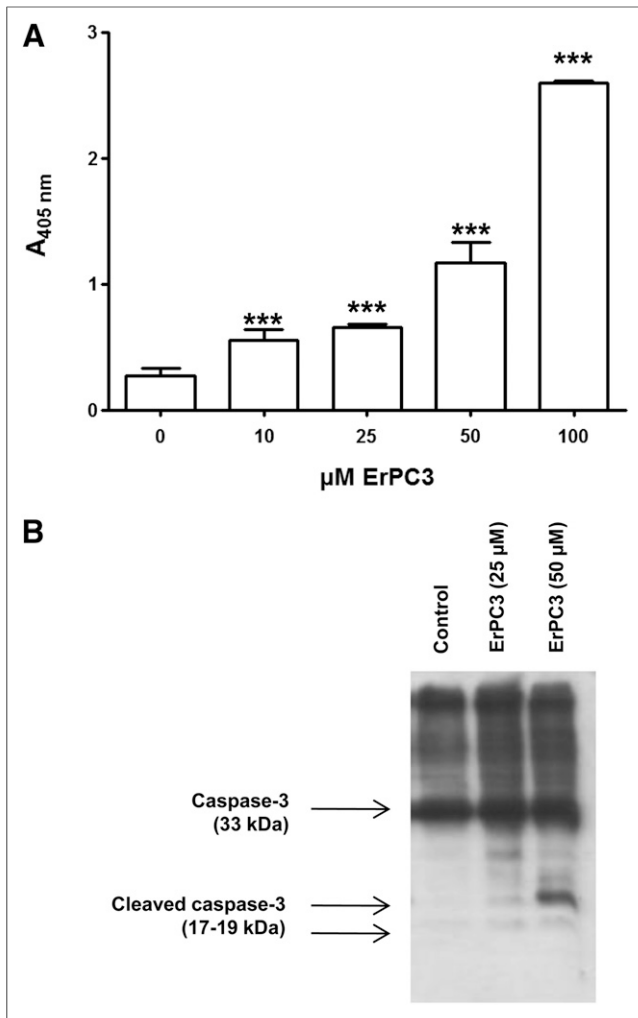


FIGURE 2. Effect of ErPC3 on apoptosis. (A) Absorbance at wavelength of 405 nm indicates level of apoptosis. Results are mean \pm SD. $***P < 0.001$, ErPC3 versus control treatment. (B) Western blot analysis of caspase-3 processing after 0, 25, and 50 μ M ErPC3 for 24 h.

were $111 \pm 75 \text{ mm}^3$ after 14 d of treatment ($n = 3$) and $203 \pm 146 \text{ mm}^3$ for mock-treated animals ($n = 4$) (Figs. 4A and 4B). Although the mean tumor volume for the control group is almost double that of the ErPC3-treated group, this difference was not statistically significant due to high interanimal variability ($P = 0.37$).

Figure 4 demonstrates specificity of ^{18}F -DPA-714 binding. Coincubation with a 5,000-fold excess of nonradiolabeled DPA-714 showed significantly reduced ^{18}F -DPA-714 binding in ErPC3- and mock-treated animals, respectively ($P < 0.0001$). ^{18}F -DPA-714 binding was also significantly lower in ErPC3- than in mock-treated animals (3.3 ± 0.4 vs. 5.2 ± 0.4 , $P < 0.001$, Figs. 4C and 4D).

For the assessment of apoptosis, brain sections were double-stained for TUNEL and TSPO. In ErPC3-treated animals, a decrease in TSPO signal correlated with TUNEL-positive areas (Fig. 5A). The ratio of TUNEL-positive area to TSPO-positive area (TUNEL+/TSPO+) was significantly higher in ErPC3-treated (17.8 ± 8.8) than in mock-treated rats (0.5 ± 0.1 ; $P < 0.0001$) (Fig. 5B).

In the brain, high levels of TSPO are mainly found in activated microglia/macrophages, activated astrocytes, and glioma cells. Thus, the ^{18}F -DPA-714 PET signal and the TSPO immunolabeling in the tumor may originate from a combination of these 3 cell types as

previously demonstrated (12). To investigate the presence of activated microglia/macrophages and astrocytes, we performed multiple immunolabeling for TSPO, CD11b, and glial fibrillary acidic protein (GFAP) as markers of glioma, activated microglia/macrophages, and astrocytes, respectively. In mock-treated rats, CD11b and GFAP signals were mainly observed in the periphery of the tumor. An increase in CD11b-positive cells within the tumor core was observed after ErPC3 treatment (Figs. 6A and 6B). Similarly, numerous GFAP-positive cells were also seen in the tumor core (Figs. 6A and 6B) of ErPC3-treated animals. At higher magnification, the ErPC3-treated rat brain sections showed costaining of CD11b-positive and GFAP-positive cells with TSPO. Colocalization of the CD11b and TSPO signal was also found in tumors of control animals, but there was no colocalization of GFAP-positive cells with TSPO-positive stain (Fig. 6C).

DISCUSSION

In 2012, the mean survival rate from glioma at the time of diagnosis was 15 mo; new treatments are urgently required. ErPC3, an alkylphosphocholine derivative, has been reported to exert proapoptotic action on glioblastoma cells. In the present study, we investigated the activity of ErPC3 on rat 9L glioma, in vitro in cell cultures, and in vivo using molecular imaging.

In cell culture, ErPC3 reduced 9L cell proliferation and viability significantly. Induction of apoptosis was demonstrated by a significant increase in DNA degradation in 9L cells and caspase-3

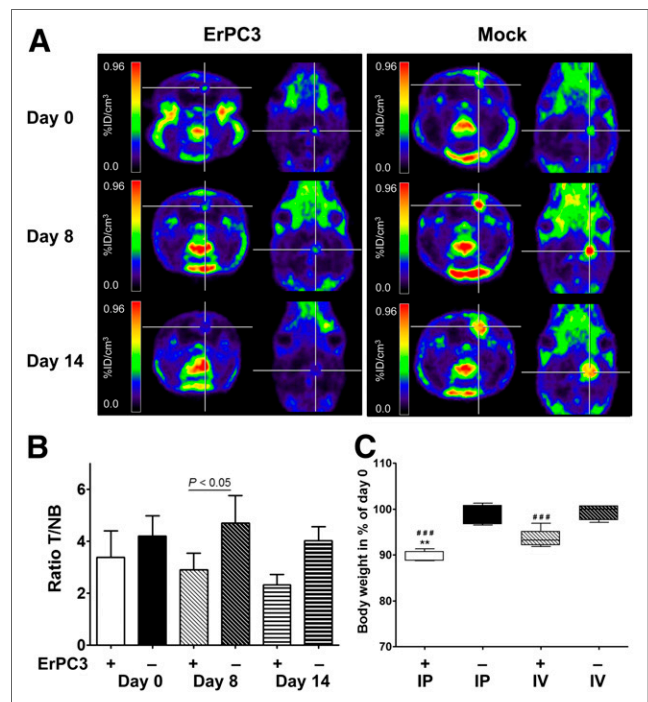


FIGURE 3. Effect of ErPC3 in vivo. (A) ErPC3 treatment reduces ^{18}F -DPA-714 tumor uptake: representative coregistered brain ^{18}F -DPA-714 PET images in ErPC3- and mock-treated animals before and during ErPC3 treatment. (B) Graphs of mean \pm SD of tumor-to-contralateral ^{18}F -DPA-714 uptake ratios for ErPC3- and control-treated animals at day 0, 8, and 14 after intraperitoneal (IP) administration. T/NB ratios show significant difference ($P < 0.05$) between 2 groups at day 8 of ErPC3 administration. (C) One week of ErPC3 treatment reduces body weight significantly ($***P < 0.001$, compared with control group). Intraperitoneal injections of ErPC3 induce more severe loss in body weight than intravenous (IV) injections ($**P < 0.01$). %ID/ cm^3 = percentage injected dose per cubic centimeter.

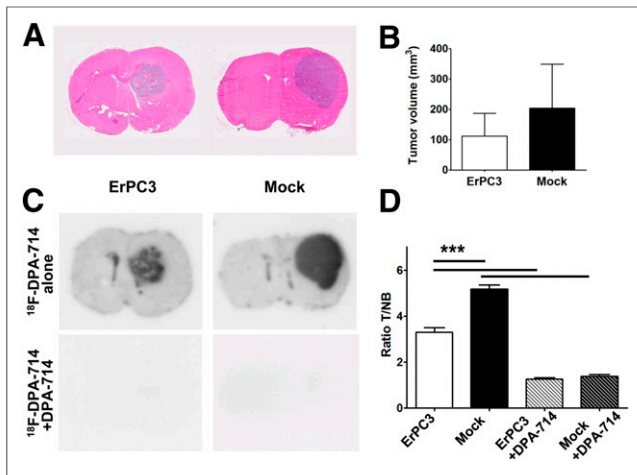


FIGURE 4. ErPC3 decreases tumor volume. (A) Hematoxylin and eosin staining of brain sections from ErPC3- and mock-treated animals. (B) Quantitative analysis using CellProfiler. Tumor volumes are smaller in ErPC3-treated than in control animals at day 14 after treatment, but this difference is not statistically significant ($P = 0.37$). (C) Autoradiography of tumor-bearing brain sections. ^{18}F -DPA-714 binding is significantly reduced in ErPC3-treated versus control animals and in presence of nonlabeled DPA-714 ($P < 0.0001$).

activation. These results are in agreement with previously published reports demonstrating that ErPC3 has antineoplastic and apoptotic effects on glioblastoma cells (15,23,30).

The positive *in vitro* results encouraged us to further explore ErPC3 as treatment for rats bearing intracranial 9L gliomas. Erdlenbruch et al. investigated the *in vitro* and *in vivo* effect of ErPC (25 mg/kg) in subcutaneous and intracerebral grafts of C6 glioma (18). They noted a positive treatment response, but only in subcutaneous tumors, whereas the intracerebral tumors showed a poor response to therapy, which they explained by a limited access of ErPC to the central nervous system leading to low concentrations of the drug in the intracranial tumors. However, other studies reported drug concentrations higher than 200 nmol/g in rat and mouse brain tissue on ErPC and ErPC3 administration at 40 mg/kg (19,20), concentrations exceeding the threshold doses of ErPC (lethal concentration 50 [LC50]; concentration required to kill 50% of a population = 29–70 μM (17) and ErPC3 (LC50 < 50 μM , this study) that induce cytotoxicity in glioma cell lines *in vitro*, suggesting that the concentration of ErPC3 reaching the intracranial 9L tumors is sufficient to induce tumor cell death.

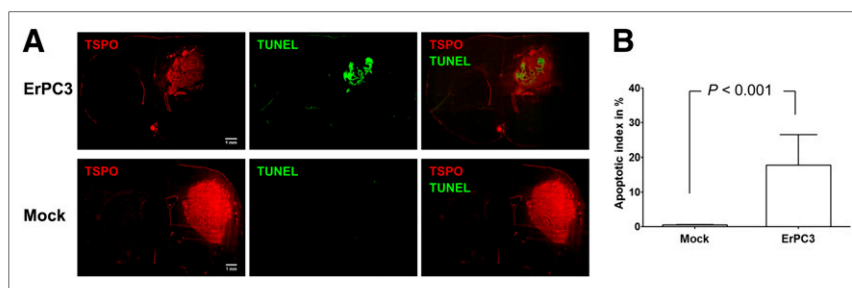


FIGURE 5. TUNEL staining in experimental gliomas. (A) Increased levels of TUNEL staining (green) in tumors of ErPC3-treated animals, compared with controls, is indicative of increased apoptosis. TSPO staining (red) shows lack of TSPO expression in some TUNEL-positive cells (combined image). (B) Quantitative evaluation of tumor area demonstrates increase in percentage of TUNEL-positive cells in ErPC3-treated animals, compared with mock-treated animals.

An alternative explanation is that Erdlenbruch et al. (18) started the ErPC treatment 11 d before tumor implantation, thus exploring the capacity of ErPC to delay tumor growth without providing any indication on its direct therapeutic activity in established tumors. Here, TUNEL staining of brain sections and *ex vivo* measurements show increased cell death (Fig. 5) and a tendency toward a decrease in mean tumor volume (Fig. 4) on ErPC3 treatment. However, the difference in the mean tumor volumes between the ErPC3-treated and control groups was not statistically significant ($P = 0.37$). Still, we cannot exclude that this lack of statistical significance could be due to the large interanimal variability (coefficient of variation = 67% and 72%) or the small sample size ($n = 3$ and 4 for treated and control groups, respectively).

It is generally accepted that changes in tumor size correlate to treatment efficacy and survival benefit. Specifically, response to treatment is often based on the Response Evaluation Criteria In Solid Tumors, which consists of the measurement of the longest dimension in the lesion for all target lesions (31). Although these criteria are useful to standardize evaluation of treatment response across different clinical trials, they fail to capture cases when a therapeutic response is achieved without significant tumor shrinkage, particularly when targeted therapies are administered and a cytostatic treatment effect is achieved (32,33). To better account for these cases, the incorporation of functional and metabolic imaging evaluation parameters has been proposed (33). For example, functional and metabolic imaging using PET, in particular ^{18}F -FDG, has extensively demonstrated its value for the evaluation of treatment response of targeted drugs and in the monitoring of early response to therapies (34). However, ^{18}F -FDG brain tumor detection is limited by high background signal in the normal brain, resulting in low tumor-to-background ratios. Radiolabeled amino acids or nucleosides such as 3'-deoxy-3'- ^{18}F -fluorothymidine (^{18}F -FLT) have also been used as predictive markers for glioma treatment response (35,36). However, the transport of thymidine analogs is restricted across the intact blood–brain barrier, limiting the use of ^{18}F -FLT for early glioma development. As TSPO expression in glioma has been correlated to malignancy, proliferation, apoptosis, and survival, it was explored as a prognostic marker (6–8). Here, PET imaging of TSPO with ^{18}F -DPA-714, a newly proposed marker for glioma detection with rapid blood–brain barrier penetration (10,12,13), was implemented and used for the assessment of treatment efficacy.

ErPC3 treatment induces a statistically significant reduction in the uptake of ^{18}F -DPA-714 in tumors. ROI analysis of the PET images shows a significantly lower level of ^{18}F -DPA-714 uptake within the tumor of drug-treated animals at day 8 ($P = 0.002$) after ErPC3 administration, compared with control animals. Accordingly, autoradiography and immunolabeling of brain sections show reduced ^{18}F -DPA-714 binding and TSPO expression, respectively, within ErPC3-treated tumors (Figs. 4 and 6), consistent with the PET data from the same animals. Likewise, TUNEL-positive areas demonstrate a decrease in TSPO signal, suggesting downregulation or degradation of TSPO in response to ErPC3 treatment. In contrast, tumor volumes are not significantly reduced in ErPC3-treated groups, compared with controls. Moreover, they are in a range

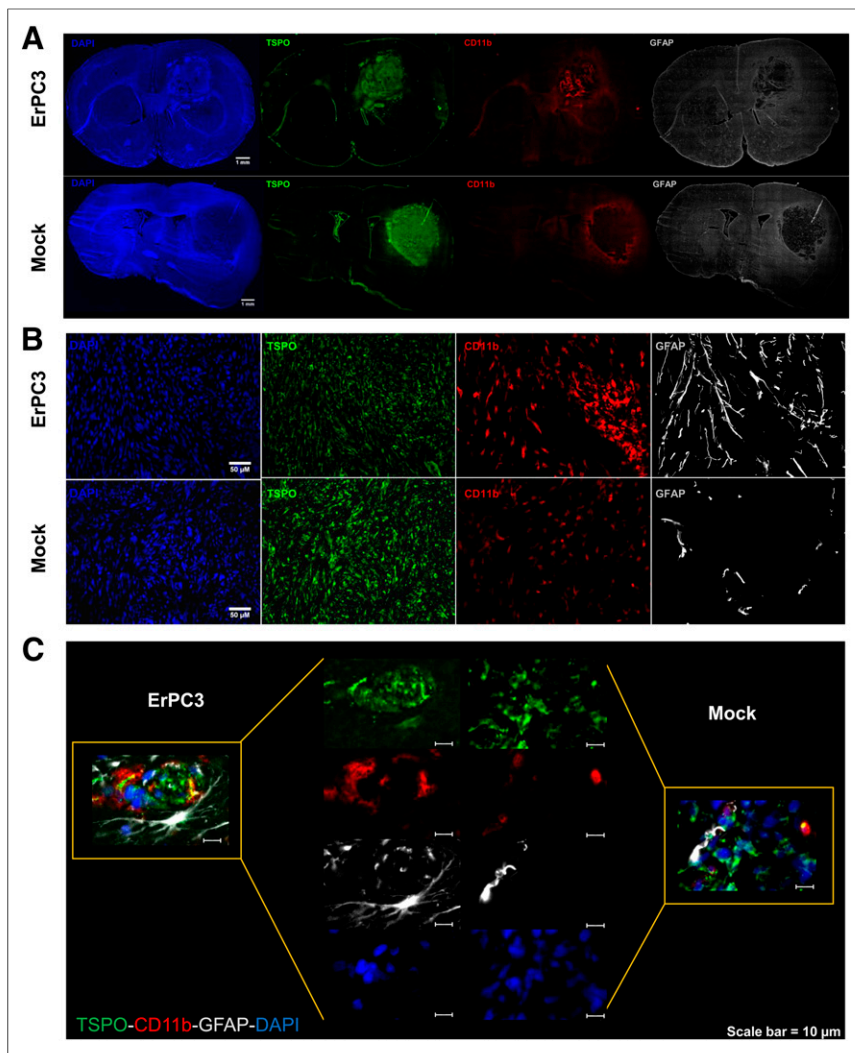


FIGURE 6. Increased infiltration of microglia and astrocytes in ErPC3-treated tumors. (A) Immunohistochemical staining of TSPO (green), CD11b (red), and GFAP (white) of whole coronal brain sections from animals bearing intracranial 9L glioma. (B) More CD11b-positive and GFAP-positive cells are found within tumor core of ErPC3-treated animals than controls. (C) TSPO expression in CD11b-positive and GFAP-positive cells in tumor core of ErPC3-treated animals is hardly detectable in control animals. DAPI = 4',6-diamidino-2-phenylindole.

most likely influenced by partial-volume effects, and thus no discrimination is feasible if the decrease in ^{18}F -DPA-714 uptake is due to a reduction in tumor volume or TSPO density. However, ^{18}F -DPA-714 binding studies and immunohistochemistry strongly support the idea of reduced TSPO tumor density after ErPC3 treatment. These results demonstrate the capacity of ^{18}F -DPA-714 as a surrogate marker for quantification of the pharmacologic activity of ErPC3 and support previous results showing that the antitumoral activity of ErPC/ErPC3s requires the expression of TSPO (15,24). It is important to note that Western blot results demonstrated high TSPO levels in the rodent glioma cell line 9L and C6, whereas TSPO expression was undetectable in murine GL261 glioma cells. Although high levels of TSPO density have been extensively reported in malignant brain tumors and successfully correlated to tumor proliferation and grade, one should also consider the existence of TSPO-negative gliomas (37).

The differences observed between the treated and untreated groups relate to the higher degree of infiltration of CD11b-positive

immune cells and GFAP-positive astrocytes in the tumors of ErPC3-treated animals with respect to control tumors (Fig. 6). The pattern of distribution of astrocytes and microglia/macrophages is highly evocative of migration of these cells to the tumor core, suggesting that inflammatory cells and astrocytes infiltrate the tumor region in response to ErPC3 treatment and tumor cell death.

The knockdown of TSPO in rat C6 glioma cells reduces significantly the induction of apoptosis and the activation of caspase-3 after treatment with ErPC3 (24). These observations have led to the hypothesis that there is a direct interaction between ErPC3 and TSPO, and our observation of a downregulation of TSPO expression after ErPC3 is in favor of this hypothesis. Furthermore, TSPO has been closely associated with the mitochondrial permeability transition pore. In fact, using cyclosporine A, recent reports have described the blockage of the mitochondrial permeability transition pore complex countering ErPC3-induced apoptosis and decreasing tumor-infiltrating microglia/macrophages (15,23,38). Therefore, interaction between ErPC3 and TSPO leading to the attraction of inflammatory cells is a plausible mechanism. However, whether TSPO is directly implicated in attracting microglia/macrophages and reactive astrocytes into the tumor remains the subject of further investigations.

The infiltration of TSPO-positive microglia/macrophages and reactive astrocytes into the tumor core suggests that the tumor microenvironment was significantly modified by ErPC3 treatment. It remains to be determined whether ErPC3 can elicit an apoptotic effect in these tumor stroma cell populations. However, it has been demon-

strated that the toxicity of ErPC3 is selectively greater toward cancer cells than toward human or mouse bone marrow cells (21) and that ErPC3 could stimulate innate immunity by inducing human cord blood cells to form granulocytes/macrophage colonies (39).

Finally, a statistically significant loss in body weight was observed in the ErPC3-treated animals ($P < 0.001$). Systemic toxicity associated with ErPC3 has been reported in nude mice (20), with intraperitoneal administration leading to a transient, tolerable (less than 10%) weight loss after 14 d of treatment with 40 mg/kg of ErPC3, a dose similar to the one used in the present study. Another study (19) on the biodistribution of the congener drug ErPC in rats reported a decline in body weight after intravenous injection of the maximum-tolerated dose of 40 mg/kg. It is important to note that the above-mentioned studies were performed in healthy animals, whereas the present study was conducted in tumor-bearing, hence more fragile, animals. In any case, differences remained statistically significant after normalization by body weight, independently of the administration route ($P < 0.05$ for intraperitoneal, $P < 0.01$ for intravenous).

CONCLUSION

PET imaging of TSPO expression using ¹⁸F-DPA-714 allows effective monitoring and quantification of disease progression and response to ErPC3 therapy in intracranial 9L gliomas. The decrease in TSPO expression is positively correlated to treatment response, extensive cell death, and infiltration by macrophage/microglia and astrocytes after ErPC3 therapy. This first, to our knowledge, in vivo demonstration of the antitumor activity of ErPC3 calls for further exploration of alkylphosphocholines as therapeutic agents in glioma.

DISCLOSURE

The costs of publication of this article were defrayed in part by the payment of page charges. Therefore, and solely to indicate this fact, this article is hereby marked "advertisement" in accordance with 18 USC section 1734. This research was funded by the European Union's Sixth and Seventh Framework Programme under grant agreement LSHB-CT-2005-512146 (DiMI), LSHC-CT-2004-503569 (EMIL), HEALTH-F2-2011-278850 (INMiND), the Joint INCa/DAAD Translational Research Program on Cancer (08-006), and a PhD Scholarship of the Ecole Doctorale 436 Université Paris-Descartes. No other potential conflict of interest relevant to this article was reported.

ACKNOWLEDGMENTS

We are grateful to Dr. Makoto Higuchi for kindly providing the anti-TSPO antibody NP155 and to Genzyme for providing Erufosine.

REFERENCES

- Papadopoulos V, Baraldi M, Guilarte TR, et al. Translocator protein (18kDa): new nomenclature for the peripheral-type benzodiazepine receptor based on its structure and molecular function. *Trends Pharmacol Sci.* 2006;27:402–409.
- Winkler A, Boisgard R, Martin A, Tavittian B. Radioisotopic imaging of neuroinflammation. *J Nucl Med.* 2010;51:1–4.
- Chen MK, Guilarte TR. Translocator protein 18 kDa (TSPO): molecular sensor of brain injury and repair. *Pharmacol Ther.* 2008;118:1–17.
- Batarseh A, Papadopoulos V. Regulation of translocator protein 18 kDa (TSPO) expression in health and disease states. *Mol Cell Endocrinol.* 2010;327:1–12.
- Galiègue S, Casellas P, Kramar A, Tinel N, Simony-Lafontaine J. Immunohistochemical assessment of the peripheral benzodiazepine receptor in breast cancer and its relationship with survival. *Clin Cancer Res.* 2004;10:2058–2064.
- Vlodavsky E, Soustiel JF. Immunohistochemical expression of peripheral benzodiazepine receptors in human astrocytomas and its correlation with grade of malignancy, proliferation, apoptosis and survival. *J Neurooncol.* 2007;81:1–7.
- Miettinen H, Kononen J, Haapasalo H, et al. Expression of peripheral-type benzodiazepine receptor and diazepam binding inhibitor in human astrocytomas: relationship to cell proliferation. *Cancer Res.* 1995;55:2691–2695.
- Rechichi M, Salvetti A, Chelli B, et al. TSPO over-expression increases motility, transmigration and proliferation properties of C6 rat glioma cells. *Biochim Biophys Acta.* 2008;1782:118–125.
- Jacobs AH, Tavittian B. Noninvasive molecular imaging of neuroinflammation. *J Cereb Blood Flow Metab.* 2012;32:1393–1415.
- James ML, Fulton RR, Vercoullie J, et al. DPA-714, a new translocator protein-specific ligand: synthesis, radiofluorination, and pharmacologic characterization. *J Nucl Med.* 2008;49:814–822.
- Abourbeh G, Theze B, Maroy R, et al. Imaging microglial/macrophage activation in spinal cords of experimental autoimmune encephalomyelitis rats by positron emission tomography using the mitochondrial 18 kDa translocator protein radioligand [¹⁸F]DPA-714. *J Neurosci.* 2012;32:5728–5736.
- Winkler A, Boisgard R, Awde AR, et al. The translocator protein ligand [¹⁸F]DPA-714 images glioma and activated microglia in vivo. *Eur J Nucl Med Mol Imaging.* 2012;39:811–823.
- Tang D, Hight MR, McKinley ET, et al. Quantitative preclinical imaging of TSPO expression in glioma using *N,N*-diethyl-2-(2-(4-(2-¹⁸F-fluoroethoxy)phenyl)-5,7-dimethylpyrazolo[1,5-a]pyrimidin-3-yl)acetamide. *J Nucl Med.* 2012;53:287–294.
- Buck JR, McKinley ET, Hight MR, et al. Quantitative, preclinical (PET) of translocator protein expression in glioma using ¹⁸F-N-fluoroacetyl-N-(2,5-dimethoxybenzyl)-2-phenoxyaniline. *J Nucl Med.* 2011;52:107–114.
- Kugler W, Veenman L, Shandalov Y, et al. Ligands of the mitochondrial 18 kDa translocator protein attenuate apoptosis of human glioblastoma cells exposed to erucylphosphocholine. *Cell Oncol.* 2008;30:435–450.
- Jendrossek V, Muller I, Eibl H, Belka C. Intracellular mediators of erucylphosphocholine-induced apoptosis. *Oncogene.* 2003;22:2621–2631.
- Jendrossek V, Erdlenbruch B, Hunold A, Kugler W, Eibl H, Lakomek M. Erucylphosphocholine, a novel antineoplastic ether lipid, blocks growth and induces apoptosis in brain tumor cell lines in vitro. *Int J Oncol.* 1999;14:15–22.
- Erdlenbruch B, Jendrossek V, Marx M, Hunold A, Eibl H, Lakomek M. Antitumor effects of erucylphosphocholine on brain tumor cells in vitro and in vivo. *Anticancer Res.* 1998;18:2551–2557.
- Erdlenbruch B, Jendrossek V, Gerriets A, Vetterlein F, Eibl H, Lakomek M. Erucylphosphocholine: pharmacokinetics, biodistribution and CNS-accumulation in the rat after intravenous administration. *Cancer Chemother Pharmacol.* 1999;44:484–490.
- Henke G, Lindner L, Vogeser M, et al. Pharmacokinetics and biodistribution of Erufosine in nude mice - implications for combination with radiotherapy. *Radiat Oncol.* 2009;4:46.
- Bagley RG, Kurtzberg L, Rouleau C, Yao M, Teicher BA. Erufosine, an alkylphosphocholine, with differential toxicity to human cancer cells and bone marrow cells. *Cancer Chemother Pharmacol.* 2011;68:1537–1546.
- Rudner J, Ruiner C-E, Handrick R, Eibl H-J, Belka C, Jendrossek V. The Akt-inhibitor Erufosine induces apoptotic cell death in prostate cancer cells and increases the short term effects of ionizing radiation. *Radiat Oncol.* 2010;5:108.
- Lemesko VV, Kugler W. Synergistic inhibition of mitochondrial respiration by anticancer agent erucylphosphocholine and cyclosporin A. *J Biol Chem.* 2007;282:37303–37307.
- Levin E, Premkumar A, Veenman L, et al. The peripheral-type benzodiazepine receptor and tumorigenicity: isoquinoline binding protein (IBP) antisense knock-down in the C6 glioma cell line. *Biochemistry.* 2005;44:9924–9935.
- Kuhnast B, Damont A, Hinnen F, et al. [¹⁸F]DPA-714, [¹⁸F]PBR111 and [¹⁸F]FEDAA1106-selective radioligands for imaging TSPO 18 kDa with PET: automated radiosynthesis on a TRACERLab FX-FN synthesizer and quality controls. *Appl Radiat Isot.* 2012;70:489–497.
- Cizek J, Herholz K, Vollmar S, Schrader R, Klein J, Heiss WD. Fast and robust registration of PET and MR images of human brain. *Neuroimage.* 2004;22:434–442.
- Lamprecht MR, Sabatini DM, Carpenter AE. CellProfiler: free, versatile software for automated biological image analysis. *Biotechniques.* 2007;42:71–75.
- Abramoff MD, Magelhaes PJ, Ram SJ. Image processing with ImageJ. *Biophotonics International.* 2004;11:36–42.
- Chauveau F, Van Camp N, Dolle F, et al. Comparative evaluation of the translocator protein radioligands ¹¹C-DPA-713, ¹⁸F-DPA-714, and ¹¹C-PK11195 in a rat model of acute neuroinflammation. *J Nucl Med.* 2009;50:468–476.
- Rübel A, Handrick R, Lindner L, et al. The membrane targeted apoptosis modulators erucylphosphocholine and erucylphosphocholine increase the radiation response of human glioblastoma cell lines in vitro. *Radiat Oncol.* 2006;1:6.
- Therasse P, Arbuck SG, Eisenhauer EA, et al. New guidelines to evaluate the response to treatment in solid tumors. *J Natl Cancer Inst.* 2000;92:205–216.
- Suzuki C, Jacobsson H, Hatschek T, et al. Radiologic measurements of tumor response to treatment: practical approaches and limitations. *Radiographics.* 2008;28:329–344.
- Wahl RL, Jacene H, Kasamon Y, Lodge MA. From RECIST to PERCIST: evolving considerations for PET response criteria in solid tumors. *J Nucl Med.* 2009;50(suppl 1):122S–150S.
- Weber WA. Positron emission tomography as an imaging biomarker. *J Clin Oncol.* 2006;24:3282–3292.
- Galldiks N, Kracht LW, Burghaus L, et al. Patient-tailored, imaging-guided, long-term temozolomide chemotherapy in patients with glioblastoma. *Mol Imaging.* 2010;9:40–46.
- Schwarzenberg J, Czernin J, Cloughesy TF, et al. 3'-deoxy-3'-¹⁸F-fluorothymidine PET and MRI for early survival predictions in patients with recurrent malignant glioma treated with bevacizumab. *J Nucl Med.* 2012;53:29–36.
- Takaya S, Hashikawa K, Turkheimer FE, et al. The lack of expression of the peripheral benzodiazepine receptor characterises microglial response in anaplastic astrocytomas. *J Neurooncol.* 2007;85:95–103.
- Gabrusiewicz K, Ellert-Miklaszewska A, Lipko M, Sielska M, Frankowska M, Kaminska B. Characteristics of the alternative phenotype of microglia/macrophages and its modulation in experimental gliomas. *PLoS ONE.* 2011;6:e23902.
- Yosifov DY, Todorov PT, Zaharieva MM, et al. Erucylphospho-N,N,N-trimethylpropylammonium (erufosine) is a potential antimyeloma drug devoid of myelotoxicity. *Cancer Chemother Pharmacol.* 2011;67:13–25.